



This is the accepted manuscript made available via CHORUS. The article has been published as:

Nonlinear phonon Hall effects in ferroelectrics: Existence and nonvolatile electrical control

Wei Luo, Junyi Ji, Peng Chen, Yang Xu, Lifa Zhang, Hongjun Xiang, and Laurent Bellaiche Phys. Rev. B **107**, L241107 — Published 26 June 2023

DOI: 10.1103/PhysRevB.107.L241107

Nonlinear phonon Hall effects in ferroelectrics: its existence and non-volatile electrical control

Wei Luo¹†, Junyi Ji²†, Peng Chen¹, Yang Xu⁶, Lifa Zhang^{3*}, Hongjun Xiang^{2,4,5*} and Laurent Bellaiche¹

¹Physics Department and Institute for Nanoscience and Engineering, University of Arkansas, Fayetteville, Arkansas 72701, USA

²Key Laboratory of Computational Physical Sciences (Ministry of Education), State Key Laboratory of Surface Physics, and Department of Physics, Fudan University, Shanghai 200433, China

³Phonon Engineering Research Center of Jiangsu Province, Center for Quantum Transport and Thermal Energy Science, Institute of Physics Frontiers and Interdisciplinary Sciences, School of Physics and Technology, Nanjing Normal University, Nanjing 210023, China

⁴Collaborative Innovation Center of Advanced Microstructures, Nanjing 210093, China ⁵Shanghai Qi Zhi Institute, Shanghai 200030, China

⁶Key Laboratory of Polar Materials and Devices (MOE), School of Physics and Electronic Science, East China Normal University, Shanghai 200241, China Corresponding author: phyzlf@njnu.edu.cn, hxiang@fudan.edu.cn

†These authors contributed equally to this work

Abstract: Nonlinear Hall effects have been previously investigated in non-centrosymmetric systems for electronic systems. However, they only exist in metallic systems and are not compatible with ferroelectrics since these latter are insulators, hence limiting their applications. On the other hand, ferroelectrics naturally break inversion symmetry and can induce a non-zero Berry curvature. Here, we show that a non-volatile electric-field control of heat current can be realized in ferroelectrics through the nonlinear phonon Hall effects. More precisely, based on Boltzmann equation under the relaxation-time approximation, we derive the equation for nonlinear phonon Hall effects, and further show that the behaviors of nonlinear Hall effects for phonons (that are bosons) are very different from nonlinear Hall effects for electrons (that are fermions). Our work therefore provides a route for electric-field control of thermal Hall current in ferroelectrics.

Introduction

Hall effects [1-4], which typically require breaking of the time reversal (TR) symmetry, have been widely studied in the past years. Recently, the nonlinear Hall effect (NHE) [5-17], which can exist without breaking TR symmetry, attracted a lot of attention. It arises from the Berry curvature dipole (BCD) [5] in an inversion-symmetry broken system. Due to the symmetry requirement of BCD, the NHE has been proposed to detect the direction of magnetic moments [18,19], electric polarization of polar metal [20] and broadband terahertz at room temperature [21]. NHE also has been extended to nonlinear thermal Hall effects [22-26], that involve electrons and magnons.

Ferroelectrics, which naturally break inversion-symmetry, have been widely investigated due to, e.g., their applications in non-volatile memory devices [27-29]. Ferroelectrics usually are insulators. However, the response of NHE (for electronic systems) to external electric fields is a Fermi liquid property [5] and can only exist in metallic systems. Hence, ferroelectrics and NHE are naturally not compatible to each other in principles. Note that Xiao et al. predicted that NHE can exist in the LiOsO3 ferroelectric metal [20], but it cannot be controlled by switching the polarization of metallic LiOsO3 which is metallic. Similarly, although ferroelectrics can also be metallic for some special two-dimensional (2D) systems with out-of-plane polarization [30-33], the switchable ability of their polarization is also very limited, except for 2D WTe₂ [30]. On the other hand, compared with electronic (Fermionic) systems, phononic (Bosonic) systems may be a good platform for controlling the nonlinear phonon Hall effect (NPHE) since it is not limited to metallic systems. A natural question thus arises, namely does the NPHE exist in ferroelectric systems? If yes, are there any differences in the temperature-dependent behavior of NHE and NPHE? Moreover, could the NPHE be switched by an external electric field? Obviously, answering these questions will not only open a new possibility for NPHE, but also may lead to thermal Hall devices integrated in ferroelectrics.

In this work, by solving the Boltzmann equation under relaxation-time approximation [34], we find that NPHE can exist in any system having broken inversion-symmetry. It is very different in nature from the NHE for electrons. For instance, the NHE for electrons are only decided by the states located near the Fermi level, while NPHE are contributed by all phonon bands. Furthermore, the nonlinear Hall conductivity for electrons increases with decreasing temperature [7,14]. In contrast, the nonlinear phonon Hall conductivity first increases with increasing temperature, and then, after reaching a maximum value at a specific temperature, decreases with further heating the system. We also find that, for three-dimensional (3D) ferroelectrics, the nonlinear phonon Hall conductivity changes its sign when the ferroelectric polarization switches. While, for 2D ferroelectrics, if the two polarization states are connected by a M_z mirror symmetry, the nonlinear phonon Hall conductivity does not change its sign due to the lack of component of Berry curvature Ω_x , Ω_y , and lack of the good quantum number k_z in 2D systems. We further find that the switching of ferroelectric polarization in 3D systems switches the Weyl chirality and topological charge of Weyl phonons.

Nonlinear phonon Hall effects

The phonon Hall effect has been previously observed in experiments [35,36]. Theoretical studies show that it is caused by the Berry curvature of phonon bands in systems with Raman spin-phonon coupling [37-39] and its Hamiltonian is non-Hermitian [40]. The phonon Hall conductivity can be expressed as [41,42]

$$\kappa_{ab} = -\frac{k_B^2 T}{\hbar V} \sum_{n, \mathbf{q}} c_2(\rho) \Omega_{n, c}(\mathbf{q})$$
 (1)

where, κ_{ab} is the phonon Hall conductivity. T and V are the temperature and materials' volume. k_B and \hbar are Boltzmann and reduced Plank constants. \boldsymbol{q} and \boldsymbol{n} are Bloch wave vector and band index for phonons. \boldsymbol{a} , \boldsymbol{b} and \boldsymbol{c} (equivalent to \boldsymbol{x} , \boldsymbol{y} , and \boldsymbol{z}) are Cartesian coordinates. ρ and Ω are distribution function and Berry curvature for phonons. Here, $c_2(\rho)[42]$ is a coefficient that depends on ρ , and which is different from the c_0 ($c_0 = \rho$) involved in NHE [5] and c_1 ($c_1 = (1+\rho)In(1+\rho) - \rho In\rho$) associated with

nonlinear (spin) Nernst effect [22,25]. For non-magnetic systems (in their equilibrium state), κ_{ab} is always zero since the integration of Berry curvature in the whole Brillouin zone (BZ) for all phonon bands vanishes. Consequently, the phonon Hall conductivity vanishes. However, for non-magnetic systems with breaking inversion-symmetry, although the integration of Berry curvature is zero in the BZ, the Berry curvature $\Omega_n(q)$ is non-zero at a specific vector q of a band n. In this case, under a temperature gradient ∇T (corresponding to the non-equilibrium state), we will show that the phonon Hall conductivity κ_{ab} can be non-zero, leading to the NPHE.

The expression of c_2 in Equation (1) is [42]

$$c_2(\rho) = (1+\rho) \left(\ln \frac{1+\rho}{\rho} \right)^2 - (\ln \rho)^2 - 2Li_2(-\rho)$$
 (2)

 Li_2 is the polylogarithm of order 2. Note that, here, we consider the non-equilibrium state which is caused by the temperature gradient ∇T . Here, ρ represents the distribution function for non-equilibrium state and we expand it as $\rho \approx \rho_0 + \rho_1$, where ρ_0 refers to the Boson-Einstein distribution function for equilibrium state, and ρ_1 is a small first-order term of the temperature gradient ∇T .

Furthermore, the Boltzmann equation can be written as [43]:

$$\frac{\partial \rho}{\partial t} = -\boldsymbol{v}_{n,q} \frac{\partial \rho}{\partial r} (\boldsymbol{q}, \boldsymbol{r}, t) - \left(\frac{d\boldsymbol{q}}{dt}\right) \frac{\partial \rho}{\partial q} (\boldsymbol{q}, \boldsymbol{r}, t) - \frac{\rho - \rho_0}{\tau_n(\boldsymbol{q})}$$
(3)

where, t and r represent the time and position vector, respectively. $v_{n,q}$ is the group velocity for band n at the q point in BZ. Assuming the system in a steady state, we have $\frac{\partial \rho}{\partial t} = 0$. Since phonons have no charge, there is no electric field force. Thus, we have $\frac{dq}{dt} = 0$. The last term of equation (3) $-\frac{\rho - \rho_0}{\tau_n(q)}$ represents the collision term. $\tau_n(q)$ represents the relaxation time for phonons, which depends on q and r. For simplicity, we consider the relaxation time approximation and write it from now on as τ . Thus, Equation (3) can be simplified (for the q component) to:

$$v_{n,a}(\mathbf{q})\frac{\partial \rho}{\partial r_a} = -\frac{\rho - \rho_0}{\tau} \tag{4}$$

Putting $\rho \approx \rho_0 + \rho_1$ into equation (4) and comparing the expansion coefficients in the first-order of temperature gradient, we get

$$\rho_1 = -\tau v_{n,a}(\mathbf{q}) \frac{\partial \rho_0}{\partial T} \frac{\partial T}{\partial r_a}$$
(5)

Putting $\rho \approx \rho_0 + \rho_1$ into equation (2), and then using equation (5), we obtain after a straightforward but tedious calculation (Details can be found in the supplementary materials [44] (see also references [45-53] therein):

$$c_2(\rho) = c_2(\rho_0) + \frac{\tau k_B}{\hbar} \left(\frac{E_{n,q} - \mu}{k_B T}\right)^3 \frac{\partial \rho_0}{\partial q_a} \frac{\partial T}{\partial r_a}$$
 (6)

Where $E_{n,q}$ and μ are the energy for band n at the \boldsymbol{q} point in the BZ and the chemical potential, respectively. For phonons, the chemical potential μ is always zero since phonons are Bosons. Putting equation (6) into equation (1), and by using $\kappa_{ab} = -\frac{k_B^2 T}{\hbar V} \sum_{n,q} c_2(\rho_0) \Omega_{n,c}(\boldsymbol{q}) = 0$ for the equilibrium state (Note that we focus on the non-magnetic system), the temperature gradient induced thermal conductivity can be written for non-equilibrium states as

$$\kappa_{ab} = -\frac{\tau \nabla_d T}{V \hbar^2} \epsilon_{abc} \sum_{\boldsymbol{q}, n} \frac{E_{n, \boldsymbol{q}}^3}{T^2} \frac{\partial \rho_0}{\partial q_d} \Omega_{n, c}(\boldsymbol{q})$$
 (7)

Here, $\frac{\partial T}{\partial r_d}$ is denoted by $\nabla_d T$ and d=(a,b,c). Since $j_a=-\kappa_{ab}\nabla_b T$, we have

$$j_{a} = \frac{\tau \nabla_{d} T \nabla_{b} T}{V \hbar^{2}} \epsilon_{abc} \sum_{\boldsymbol{q}, n} \frac{E_{n, \boldsymbol{q}}^{3}}{T^{2}} \frac{\partial \rho_{0}}{\partial q_{d}} \Omega_{n, c}(\boldsymbol{q})$$
(8)

where ϵ_{abc} is the Levi-Civita symbol. One can see that the thermal current j_a (related with phonons) is proportional to the second order of the temperature gradient. Hence, we name this effect as the NPHE. Note that, in reality, the phonon relaxation time τ will be q (also n with n being the band index of phonon spectrum) dependent, i.e.

 $\tau_n(\boldsymbol{q})$. The low-frequency phonon has a longer relaxation time than the high-frequency phonon, but the energy of the low-frequency phonon is lower than that of the high-frequency phonon. These facts indicate that both low- and high-frequency phonons can have a significant contribution to the nonlinear phonon Hall effects. However, since the magnitude of the nonlinear phonon Hall effect is proportional to the first power of $\tau_n(\boldsymbol{q})$ and is proportional to the third power of $E_{n,\boldsymbol{q}}$, the high-frequency phonons would have more contribution than low-frequency phonons.

For NHE of electrons, at the equilibrium state, $\int_q c_0(f_0)\Omega$ (In this case, $c_0=f_0$ is the Fermi-Dirac distribution for equilibrium state) equals to zero for non-magnetic systems. Hence, by integration by parts, one gets $\int_q \frac{\partial f_0}{\partial q} \Omega = -\int_q f_0 \frac{\partial \Omega}{\partial q}$. The right side $-\int_q f_0 \frac{\partial \Omega}{\partial a}$ is the so-called BCD since it is related with the gradient of Berry curvature in the BZ. However, in our case, at the equilibrium state, we have $\int_q c_2(\rho_0)\Omega =$ 0 (The form of $c_2(\rho_0)$ is shown in Eq. (2)) instead of $\int_q c_0 \Omega = 0$ for non-magnetic system. Hence, we cannot use the BCD to describe the nonlinear thermal current for phonons. However, we still can define a similar pseudotensorial quantity P_{ab} = $\frac{1}{VT^2}\sum_{\boldsymbol{q},n}E_{n,\boldsymbol{q}}^3\frac{\partial\rho_0}{\partial q_n}\Omega_{n,b}(\boldsymbol{q})$ which has the same transformation properties as BCD under symmetry operations. Since ρ_0 is an even function under TR symmetry, the transformation properties under crystal symmetry of P_{ab} is only decided by q and Ω which is the same as BCD. Note that we have a factor $\frac{E_{n,q}^3}{T^2}$ for the pseudotensorial quantity P_{ab} , which is different from the factor $\frac{(E_{n,q}-\mu)^2}{T^2}$ for nonlinear anomalous Nernst effect [22]. Moreover, and as different from the nonlinear anomalous Nernst effect and NHE for electrons [5], the factor $\frac{\partial \rho_0}{\partial q_a}$ in P_{ab} indicates that the nonlinear thermal current [Equation (8)] is contributed by all phonon bands instead of the states near the Fermi level since phonons are bosons. For 3D systems, different from the BCD which is dimensionless, the pseudotensorial quantity P_{ab} has a unit of $eV * k_B^2$. While, for 2D systems, P_{ab} has a unit of $eV * k_B^2 * Å$.

Switchable NPHE in 3D ferroelectrics

In this part, we will show that, due to the symmetry requirement of the pseudotensorial quantity $P_{ab} = \frac{1}{VT^2} \sum_{q,n} E_{n,q}^3 \frac{\partial \rho_0}{\partial q_a} \Omega_{n,b}(q)$, the NPHE must change its sign when the polarization of a 3D ferroelectric is reversed. For a 3D ferroelectric, there must exist a polar axis. For simplicity, we assume it is along the +c direction. Thus, the mirror symmetry M_c is broken by the polarization, and one can then show that P_{ab} must be non-zero. Hence, one can see that the ferroelectric polarization is highly related with the symmetry of the pseudotensorial quantity P_{ab} . When the polarization is switched, the structure is reflected by inversion symmetry. Under inversion symmetry, Ω_b is even and q_a is odd (Note that ρ_0 is even under TR symmetry). Thus, the P_{ab} must reverse its sign when the polarization is reverted. More interestingly and since the Berry curvature does not change sign under inversion symmetry, the Weyl chirality and topological charge of Weyl points for 3D ferroelectrics should reverse their sign when switching the electrical polarization of 3D ferroelectrics. Related details of such features can be found in Supplemental Material [44].

We then take the 3D ferroelectric PbTiO₃[54] as an example and explain how the NHPE can be controlled by switching the polarization. The crystal structure of PbTiO₃ is shown in Fig. 1(a). It is a tetragonal phase with the *P4mm* space group (number 99) and C_{4v} point group. This latter point group implies that the pseudotensorial quantity P_{ab} has the form (see Supplemental Material [44]) of

$$\begin{bmatrix} 0 & P_{xy} & 0 \\ -P_{xy} & 0 & 0 \\ 0 & 0 & 0 \end{bmatrix}$$

For which only P_{xy} and P_{yx} are non-zero. Based on equation (8), we have

$$j_{z} = \frac{\tau(\nabla_{x}T)^{2}}{V\hbar^{2}} \sum_{\boldsymbol{q},n} \frac{E_{n,\boldsymbol{q}}^{3}}{T^{2}} \frac{\partial \rho_{0}}{\partial a_{x}} \Omega_{n,y}(\boldsymbol{q}) = \frac{\tau(\nabla_{x}T)^{2}}{\hbar^{2}} P_{xy}$$

$$\tag{9}$$

This equation implies that, for PbTiO₃ with a polarization down, adding a temperature gradient $(\nabla_x T)$ along the -x direction will induce a thermal current (along the -z direction) that is proportional to both $(\nabla_x T)^2$ and P_{xy} (P_{xy} is positive for a polarization down with temperature higher than 30 Kelvin (K)) [see Fig. 1(a)]. After the polarization is switched by an electric field, the nonlinear thermal current j_z switches its sign due to the change of sign of P_{xy} , while the temperature gradient is maintained.

We calculate the P_{xy} as a function of temperature for PbTiO₃, and the results are shown in Fig. 1(c). When the temperature is low (that is, lower than 20K, see Fig. 1(c)), the magnitude of P_{xy} is small. With increasing temperature, the magnitude of P_{xy} quickly increases (between 20K and 80K). In the high temperature limit, the magnitude of P_{xy} decreases again. As indicated in Fig. 1(c), reverting the polarization direction results in the P_{xy} being reversed. The behaviors of the P_{xy} as a function of temperature, and detailed calculations for P_{xy} can be seen Supplemental Material [44]. We also investigated the component P_{xy} as a function of frequency (the chosen range of frequency for PbTiO₃ is from 0 THz to 25 THz since the maximum frequency is around 24 THz), see Supplemental Material [44]). The result is shown in Fig. 1(d). The temperature is fixed at either $k_BT=2.6\ meV$ (which corresponds to 30 K) or $k_BT=$ 18.1 meV (corresponding to 210 K). Comparing the result for these two different temperatures, one can see that, at low temperature, only low-frequency phonon bands make contribution for P_{xy} ; the high-frequency phonons being thus frozen. On the other hand, for higher temperature, the high-frequency phonons are excited and have significant contribution for P_{xy} , implying that is contributed by all phonon bands. Due to the cancellation of the Berry curvature for different phonon bands, P_{ab} can change its sign for different frequency values. Note also that P_{ab} at frequency w is calculated by using $P_{ab} = \frac{1}{VT^2} \sum_{w} \sum_{q,n} E_{n,q}^3 \frac{\partial \rho_0}{\partial q_a} \Omega_{n,b}(q)$ and summing over the states between 0 THz and w THz (w is the frequency of phonons). To make sure that the computed Berry curvature is converged, we tested the results for different q grids (see Supplemental Material [44]). The results are shown in Supplemental Material [44].

NPHE in 2D ferroelectrics

For 2D systems, the Berry curvature just has a finite component for Ω_z . The good quantum number for q are q_x and q_y . Hence, only P_{xz} and P_{yz} can be defined. For this reason, the switching of the electrical polarization of a 2D ferroelectric will not always changes the sign of the NPHE. Specifically, a 2D ferroelectric only maintaining an outof-plane polarization (e.g., along +z) cannot realize the sign reversal of the nonlinear thermal current. In fact, for a 2D ferroelectric only maintaining an out-of-plane polarization is such as its two polarization states are connected by a mirror symmetry M_z , with Ω_z , q_x and q_y all being even under the M_z operation. Thus, P_{xz} and P_{yz} do not change their sign when changing the polarization. One specific example is the monolayer CuInP₂S₆ for which the two ferroelectric states (with only out-of-plane polarization) are connected by M_z [55,56]. The phonon spectra are shown in Supplemental Material [44], and the phonon berry curvature distribution for the two ferroelectric states can be found in Supplemental Material [44]. On the other hand, a 2D ferroelectric only maintaining an in-plane polarization [e.g., along +y(+x)] can realize the sign reversal of the NPHE since its two polarization states are connected by a mirror symmetry M_{ν} (M_{x}). Ω_{z} being odd under the M_{ν} (M_{x}) operation while q_{x} (q_{ν}) is even under the M_y (M_x) operation, P_{xz} (P_{yz}) changes its sign when reverting the polarization. One example is 2D ferroelectric SnTe [57] that only has an in-plane polarization (the phonon spectra are shown in Supplemental Material [44]). Note that the point group of monolayer SnTe is C_{2v} , for which there is a mirror symmetry M_x whose normal is perpendicular to the x axis (See Fig.2 (a)). Due to such mirror symmetry M_x , P_{yz} vanishes and only P_{xz} is nonzero. This nonzero P_{xz} implies that, if there exist a temperature gradient along -x ($\nabla_x T$) direction, a nonlinear thermal current will emerge along the +y direction (since P_{xy} is negative for a polarization down (P -)with temperature higher than 40 K [see Fig. 2(c)]) which is proportional to $(\nabla_x T)^2$ (see Fig. 2(a)). Switching the polarization will reverse the direction of nonlinear thermal current j_y (see Fig. 2(b)). The P_{xz} (for both P+ and P- up and down polarization states, respectively) as a function of temperature and frequency are shown in Fig. 2(c)

and Fig. 2(d). Note that these results originate from the use of $P_{ab} = \frac{1}{VT^2} \int_0^w \sum_{q,n} E_{n,q}^3 \frac{\partial \rho_0}{\partial q_a} \Omega_{n,b}(q)$ and that the ferroelectric transition temperature for monolayer SnTe is 275 K [57], while the range of frequency for SnTe is from 0THz to 5THz (see Supplemental Material [44]). For the 2D ferroelectrics with both in-plane and out-of-plane polarization, the nonlinear phonon Hall current can also be reverted since they have non-zero in-plane component polarization. One particular example is the 2D ferroelectric In₂Se₃[58].

Discussions

Here, we roughly estimate the magnitude of NPHE, and discuss the experimental details for observing it. The experimental set-up is shown in Fig. 3. The left side (yellow cylinder) is a heater. The length, width and height of the sample are represented by l_x , l_z and l_y , respectively. Once the system reaches a steady state, we have

$$\kappa_{xz}\nabla_x T = -\kappa_{xx}\nabla_z T \tag{10}$$

Hence,
$$\nabla_z T = -\frac{\kappa_{xz}\nabla_x T}{\kappa_{xx}}$$
, i.e. $\frac{\Delta_z T}{l_z} = -\frac{\kappa_{xz}\nabla_x T}{\kappa_{xx}}$. Then, we get

$$\Delta_z T = \frac{j_z l_z}{\kappa_{xx}} \tag{11}$$

where j_z is the nonlinear Hall current and κ_{xx} is the longitudinal thermal conductivity. $\nabla_z T$ and $\nabla_x T$ are the temperature gradients along the z and x direction, respectively. $\Delta_z T$ is the temperature difference between the two sides (along the z direction) of the sample which can be directly measured. Equation (11) indicates the temperature difference $\Delta_z T$ can be enhanced by increasing j_z and l_z , and decreasing κ_{xx} . Based on Equation (9), $j_z = \frac{\tau(\nabla_x T)^2}{Vh^2} \sum_{q,n} \frac{E_{n,q}^3}{T^2} \frac{\partial \rho_0}{\partial q_x} \Omega_{n,y}(q) = \frac{\tau(\nabla_x T)^2}{h^2} P_{xy}$, one can see j_z is linear proportional to τ and tensor P_{xy} , and is quadratically proportional to $\nabla_x T$. By setting appropriate values for τ , P_{xy} and $\nabla_x T$, i.e. $\tau = 5ps$, $P_{xy} = 0.5meV * k_B^2$ (the temperature of the system is set to be 100K) and $\nabla_x T = 5K/mm$, we get $j_z = 1.71 \times 10^{-4}W * m^{-2}$. Choosing l_z to be around 1cm, and recalling that κ_{xx} for ultra-low thermal conductivity can be small as $\sim 10^{-2}W * m^{-1} * K^{-1}[59]$, we get from equation

(11), a temperature difference $\Delta_z T = \frac{j_z l_z}{\kappa_{xx}} = \frac{1.71 \times 10^{-4} \times 10^{-2}}{10^{-2}} = 1.71 \times 10^{-4} \text{K} = 0.171 m\text{K} = 117 \mu\text{K}$. This value is observable since resolution of temperature difference can be as small as $\sim 10^1 \mu\text{K}$ [60]. Moreover, if the temperature gradient $\nabla_x T$ is 10 K/mm, the temperature difference $\Delta_z T$ can be four times bigger, i.e. $468 \mu\text{K}$. Furthermore, if the sample can be grown longer along the z direction, for example, $l_z = 2cm$, $\Delta_z T$ will become as twice as large, that is $\sim 1 m\text{K}$.

Conclusions

In this work, we investigated the nonlinear phonon Hall effects based on the Boltzmann equation under relaxation-time approximation and compared differences between NHE and NPHE. Due to the looser requirement (nonlinear phonon Hall effects can occur in insulators), the nonlinear phonon Hall current and the Weyl chirality of phonons (topological charge) can be reversed by switching the ferroelectric polarization. We hope that these predictions will be observed by experiments soon and will be used to design novel quantum phononics devices.

Acknowledgements

The work is supported by the Vannevar Bush Faculty Fellowship (VBFF) grant no. N00014-20-1-2834 from the Department of Defense. Yang Xu is supported by the NSFC (12274125) and the Shanghai Pujiang Program (21PJ1403100). Lifa Zhang is supported by NSFC (11975125, 11890703). Junyi Ji and Hongjun Xiang are supported by NSFC (11825403, 12188101). These simulations were done using the Arkansas High Performance Computing Center. We thank Dr. L.Y.Gao for helpful discussions.

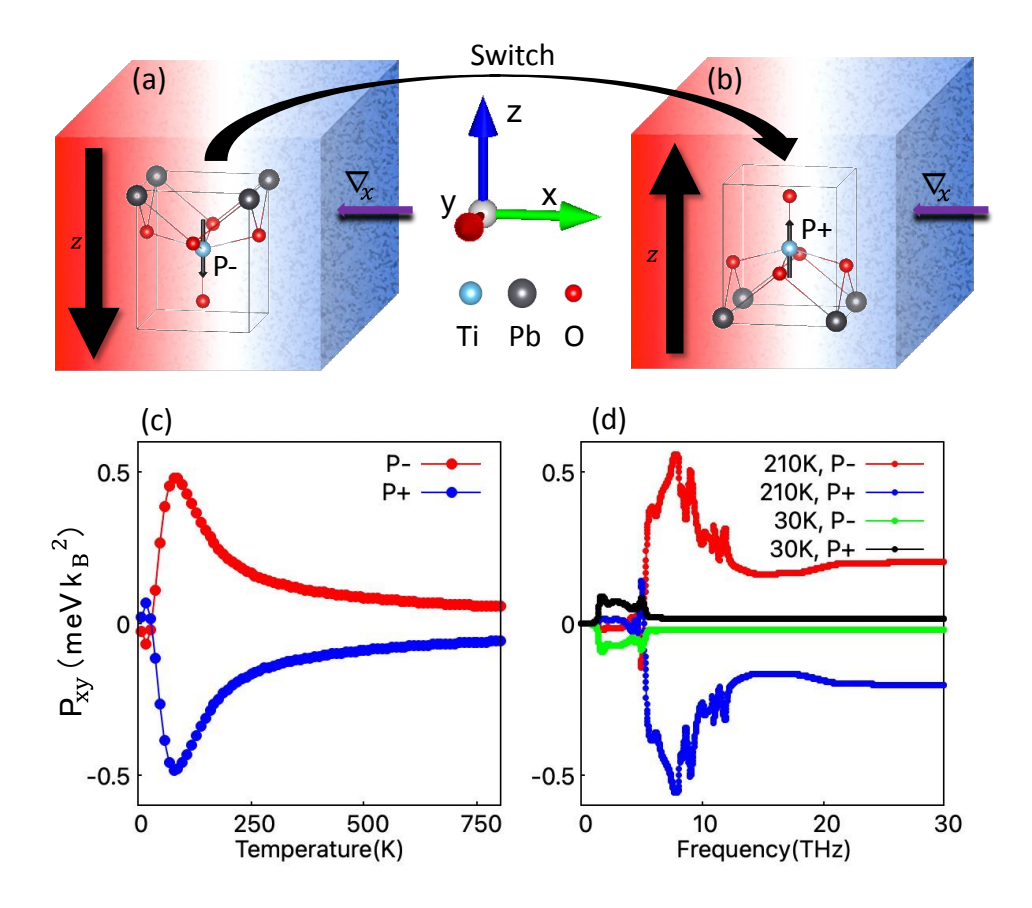


FIG. 1. Schematic diagram for the electric field control nonlinear thermal current in PbTiO₃ with polarization down state (a) and polarization up state (b). Red and blue regions indicate the hot and cold regions, respectively. P - and P + are used to label the polarization down and polarization up state. (c) P_{xy} (symmetrized) as a function of temperature. (d) P_{xy} (symmetrized) as a function of frequency.

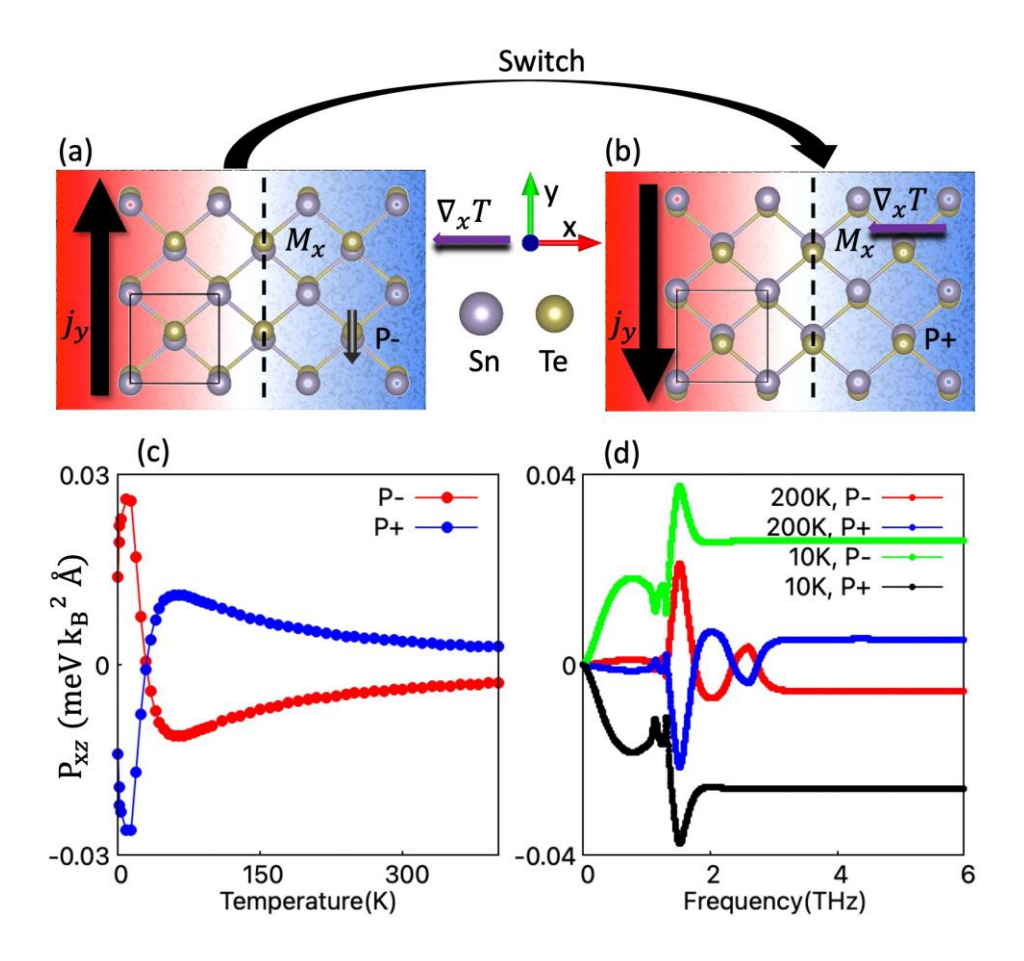


FIG.2. Schematic diagram for the electric field control nonlinear thermal current in 2D SnTe with polarization down state (a) and polarization up state (b). The black solid square line indicates the unit cell. The black dashed line represents the M_x mirror symmetry. Red and blue region represent the hot and cold regions. The P- and P+ states are connected by the M_y mirror symmetry. (c) P_{xz} (symmetrized) as a function of temperature. (d) P_{xz} (symmetrized) as a function of frequency.

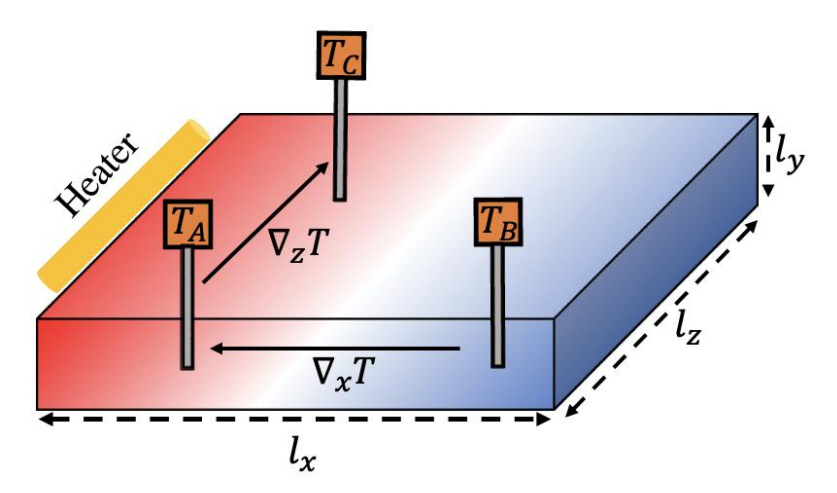


FIG. 3 Schematic diagram for experimental set-ups. The length, width and height of the sample are represented by l_x , l_z and l_y , respectively. The transverse temperature difference $\Delta_z T = T_C - T_A$.

References

- [1] N. Nagaosa, J. Sinova, S. Onoda, A. H. MacDonald, and N. P. Ong, Reviews of modern physics **82**, 1539 (2010).
- [2] K. v. Klitzing, G. Dorda, and M. Pepper, Physical review letters 45, 494 (1980).
- [3] D. Xiao, M.-C. Chang, and Q. Niu, Reviews of modern physics 82, 1959 (2010).
- [4] C. Z. Chang, J. S. Zhang, X. Feng, J. Shen, Z. C. Zhang, M. H. Guo, K. Li, Y. B.
- Ou, P. Wei, L. L. Wang et al., Science **340**, 167 (2013).
- [5] I. Sodemann and L. Fu, Physical review letters 115, 216806 (2015).
- [6] Q. Ma, S. Y. Xu, H. Shen, D. MacNeill, V. Fatemi, T. R. Chang, A. M. Valdivia, S. F. Wu, Z. Z. Du, C. H. Hsu *et al.*, Nature **565**, 337 (2019).
- [7] K. Kang, T. Li, E. Sohn, J. Shan, and K. F. Mak, Nature materials 18, 324 (2019).
- [8] S.-Y. Xu, Q. Ma, H. T. Shen, V. Fatemi, S. F. Wu, T.-R. Chang, G. Q. Chang, A.
- M. Valdivia, C.-K. Chan, Q. D. Gibson et al., Nature Physics 14, 900 (2018).
- [9] Z. Z. Du, C. M. Wang, H.-Z. Lu, and X. C. Xie, Physical Review Letters **121**, 266601 (2018).
- [10] Y. Zhang, J. van den Brink, C. Felser, and B. Yan, 2D Materials 5, 044001 (2018).
- [11] S. S. Tsirkin, P. A. Puente, and I. Souza, Physical Review B 97, 035158 (2018).
- [12] S. Singh, J. Kim, K. M. Rabe, and D. Vanderbilt, Physical review letters 125, 046402 (2020).
- [13] J.-S. You, S. Fang, S.-Y. Xu, E. Kaxiras, and T. Low, Physical Review B **98**, 121109(R) (2018).
- [14] Z. He and H. Weng, npj Quantum Materials 6, 1 (2021).
- [15] Z. Du, H.-Z. Lu, and X. Xie, Nature Reviews Physics 3, 744 (2021).
- [16] C. Wang, Y. Gao, and D. Xiao, Physical Review Letters 127, 277201 (2021).
- [17] H. Liu, J. Zhao, Y.-X. Huang, W. Wu, X.-L. Sheng, C. Xiao, and S. A. Yang, Physical Review Letters **127**, 277202 (2021).
- [18] D.-F. Shao, S.-H. Zhang, G. Gurung, W. Yang, and E. Y. Tsymbal, Physical Review Letters **124**, 067203 (2020).
- [19] C. Chen, H. Wang, Z. Yang, and H. Zhang, Chinese Physics Letters **38**, 057302 (2021).
- [20] R.-C. Xiao, D.-F. Shao, W. Huang, and H. Jiang, Physical Review B **102**, 024109 (2020).
- [21] Y. Zhang and L. Fu, Proceedings of the National Academy of Sciences 118, e2100736118 (2021).
- [22] X.-Q. Yu, Z.-G. Zhu, J.-S. You, T. Low, and G. Su, Physical Review B **99**, 201410(R) (2019).
- [23] C. Zeng, S. Nandy, A. Taraphder, and S. Tewari, Physical Review B **100**, 245102 (2019).
- [24] R. Nakai and N. Nagaosa, Physical Review B 99, 115201 (2019).
- [25] H. Kondo and Y. Akagi, Physical Review Research 4, 013186 (2022).
- [26] E. Parsonnet, L. Caretta, V. Nagarajan, H. Zhang, H. Taghinejad, P. Behera, X.
- Huang, P. Kavle, A. Fernandez, D. Nikonov *et al.*, Physical Review Letters **129**, 087601 (2022).

- [27] J. F. Scott and C. A. P. De Araujo, Science **246**, 1400 (1989).
- [28]O. Auciello, J. F. Scott, and R. Ramesh, Physics today 51, 22 (1998).
- [29] K. Uchino, Ferroelectric devices (CRC press, 2018).
- [30] Z. Fei, W. Zhao, T. A. Palomaki, B. Sun, M. K. Miller, Z. Zhao, J. Yan, X. Xu, and D. H. Cobden, Nature **560**, 336 (2018).
- [31] W. Luo, K. Xu, and H. Xiang, Physical Review B 96, 235415 (2017).
- [32] J. Lu, G. Chen, W. Luo, J. Íñiguez, L. Bellaiche, and H. Xiang, Physical Review Letters **122**, 227601 (2019).
- [33] X. Duan, J. Huang, B. Xu, and S. Liu, Materials Horizons 8, 2316 (2021).
- [34] G. D. Mahan, Many-particle physics (Springer Science & Business Media, 2013).
- [35] C. Strohm, G. L. J. A. Rikken, and P. Wyder, Physical review letters 95, 155901 (2005).
- [36] A. V. e. Inyushkin and A. Taldenkov, Jetp Letters **86**, 379 (2007).
- [37] L. Zhang, J. Ren, J.-S. Wang, and B. Li, Physical review letters **105**, 225901 (2010).
- [38] L. Zhang, J. Ren, J.-S. Wang, and B. Li, Journal of Physics: Condensed Matter **23**, 305402 (2011).
- [39] T. Qin, J. Zhou, and J. Shi, Physical Review B 86, 104305 (2012).
- [40] Y. Liu, Y. Xu, S.-C. Zhang, and W. Duan, Physical Review B 96, 064106 (2017).
- [41] L. Zhang, New Journal of Physics 18, 103039 (2016).
- [42] R. Matsumoto and S. Murakami, Physical review letters 106, 197202 (2011).
- [43]G. Mahan, (Kluwer Academic, 2000).
- [44] See Supplemental Material at http://link.aps.org/supplemental/10.1103/PhysRevLett.130.046201 for details for obtaining equation (6) in the main text; details of calculation methods; Reversing the Weyl chirality and topological charge of Weyl phonon points in 3D ferroelectric BaTiO₃; Pseudotensorial matrix from symmetry analysis; phonon spectra for 3D PbTiO₃, 2D CuInP₂S₆ and 2D SnTe; phonon Berry curvatures for 2D CuInP₂S₆ and 2D SnTe.
- [45] A. A. Mostofi, J. R. Yates, Y.-S. Lee, I. Souza, D. Vanderbilt, and N. Marzari, Computer physics communications **178**, 685 (2008).
- [46] Q. Wu, S. Zhang, H.-F. Song, M. Troyer, and A. A. Soluyanov, Computer Physics Communications **224**, 405 (2018).
- [47] J. X. Li, J. X. Liu, S. A. Baronett, M. F. Liu, L. Wang, R. H. Li, Y. Chen, D. Z. Li, Q. Zhu and X. Q. Chen, Nature communications 12, 1 (2021).
- [48] V. Bhide, K. Deshmukh, and M. Hegde, Physica 28, 871 (1962).
- [49] P. E. Blöchl, Physical review B **50**, 17953 (1994).
- [50]G. Kresse and J. Furthmüller, Physical review B 54, 11169 (1996).
- [51] G. Kresse and D. Joubert, Physical review b **59**, 1758 (1999).
- [52] J. P. Perdew, K. Burke, and M. Ernzerhof, Physical review letters 77, 3865 (1996).
- [53] A. Togo and I. Tanaka, Scripta Materialia 108, 1 (2015).
- [54] R. E. Cohen, Nature 358, 136 (1992).
- [55] A. Belianinov, Q. He, A. Dziaugys, P. Maksymovych, E. Eliseev, A. Borisevich,
- A. Morozovska, J. Banys, Y. Vysochanskii and S. V. Kalinin, Nano letters 15, 3808

- (2015).
- [56] F. C. Liu, L. You, K. L. Seyler, X. B. Li, P. Yu, J. H. Lin, X. W. Wang, J. D. Zhou, H. Wang, H. Y. He *et al.*, Nature communications **7**, 1 (2016).
- [57] K. Chang, J. W. Liu, H. C. Lin, N. Wang, K. Zhao, A. Zhang, F. Jin, Y. Zhong, X. P. Hu, W. H. Duan *et al.*, Science **353**, 274 (2016).
- [58] W. Ding, J. Zhu, Z. Wang, Y. Gao, D. Xiao, Y. Gu, Z. Zhang, and W. Zhu, Nature communications 8, 1 (2017).
- [59] C. Chiritescu, D. G. Cahill, N. Nguyen, D. Johnson, A. Bodapati, P. Keblinski, and P. Zschack, Science **315**, 351 (2007).
- [60] P. Czajka, T. Gao, M. Hirschberger, P. Lampen-Kelley, A. Banerjee, N. Quirk, D. G. Mandrus, S. E. Nagler, and N. P. Ong, Nature Materials **22**, 36 (2023).